Topochemistry of Carboxylated Cellulose Nanocrystals Resulting from TEMPO-Mediated Oxidation

Suzelei Montanari,* Mohamad Roumani, Laurent Heux, and Michel R. Vignon*

Centre de Recherches sur les Macromolécules Végétales (CERMAV-CNRS), Grenoble Cedex 9 France, and Université Joseph Fourier, BP 53, 38041, Grenoble Cedex 9, France

Received August 3, 2004; Revised Manuscript Received September 24, 2004

ABSTRACT: Surface carboxylated cellulose nanocrystals with different sizes and degrees of oxidation were prepared by TEMPO-mediated oxidation of cotton linters and microfibrils of parenchyma cell cellulose (PCC). The size of the oxidized crystals depended on (i) the starting material, (ii) an eventual acid prehydrolysis, and (iii) the oxidation conditions. The oxidized cellulose nanocrystals were characterized by transmission electron microscopy, conductometric titration, and solid-state NMR spectroscopy. During TEMPO oxidation, the main reaction corresponded to a selective oxidation of surface primary hydroxyl groups into carboxylic groups. At the same time, a decrease of the crystal size occurred, resulting from some degradation in the amorphous areas of the starting material. The introduction of negative charges at the interface of the crystalline domains induced a better individualization of the crystallites. The degrees of oxidation (DO) determined by conductometric titration were in agreement with those deduced from solid-state NMR data. The DO values reached 0.4 and 0.24 for PCC microfibrils and cotton linters, respectively. In the case of HCl-hydrolyzed samples, these values reached 0.23 for PCC microfibrils and 0.15 for cotton linters. When dispersed in water, these carboxylated cellulose crystallites led to birefringent suspensions that did not flocculate nor sediment, due to their polyelectrolyte character created by the presence of surface negative charges.

Introduction

Native cellulose is a structural material that is biosynthesized as microfibrils by a number of living organisms ranging from higher and lower plants, to some ameobae, sea animals, bacteria, and fungi.[1,2] In plant cells, the organization of the microfibrils is different in the primary and secondary wall. In the former, the microfibrils are organized in a random interwoven network consisting of individual elements associated in bundles, whereas in the latter the microfibrils are laid in parallel mode, yielding a layerlike organization. Depending on their origin, individual cellulose microfibrils have diameters from 2 to 20 nm, while their length can reach several tens of microns. Some imperfections, such as twists or kinks,[3] referred to as amorphous zones, along the microfibril length are hydrolyzed by acid treatment to produce nanocrystals sometimes called cellulose whiskers.[4−6] The shape and size of cellulose nanocrystals are more or less fixed by their origin: different samples such as tunicin, cotton, wood fibers, bacterial cellulose, parenchyma cell cellulose, etc. will produce different sizes of nanocrystals even under similar hydrolysis conditions.

Hydrolysis of cellulose with sulfuric acid under controlled conditions gives stable colloidal suspensions of cellulose nanocrystals, the properties of which depend on the cellulose source and the preparation conditions, such as reaction temperature and time, etc.[7] When the suspension concentrations exceed a critical value, the suspensions form chiral nematic ordered phases.[6−11] While the cellulose nanocrystal suspensions resulting from sulfuric acid hydrolysis are stabilized via an electrostatic repulsion induced by surface charge resulting from the introduction of sulfate esters groups,[9] those resulting from hydrochloric acid have minimal surface charges and show some important differences from the former, namely, flocculation and anomalous viscosity.[12,13]

Parenchyma cell cellulose (PCC) microfibril suspensions prepared with a Manton−Gaulin apparatus give stable colloidal suspensions without any treatment with sulfuric acid.[14,15] These cellulose suspensions are indeed stabilized by the presence of glucuronic and galacturonic acid residues at the surface of the microfibrils, as already published.[16,17]

Stable colloidal aqueous suspension of HCl-hydrolyzed cellulose nanocrystals can also be prepared by postsulfating[12,13,18] or by carboxylation and grafting of poly(ethylene glycol) with a terminal amino group.[19] In this latter case, the precise location of the carboxylation sites has not been addressed.

To prepare suspensions of cellulose nanocrystals of improved stability and to get better insights in the topochemistry of mild cellulose oxidation, we have oxidized cotton linters and PCC microfibrils from sugar beet pulp (SBP) before and after HCl-hydrolysis, using the TEMPO technique.[20−25] This oxidation method uses a mixture of sodium hypochlorite, sodium bromide, and 2,2,6,6-tetramethyl-1-piperidinyloxy radical (TEMPO). With such reagents, the oxidation is selective as it oxidizes exclusively the primary hydroxyl groups while leaving untouched the secondary ones.[21,23] The TEMPO oxidation has been applied to cellulose, leading to partial or complete solubilization depending on the crystalline nature of the starting material. Regenerated cellulose (cellulose II)[26,27] and cellulose III[25] presented crystalline structures with primary hydroxyl groups relatively accessible and therefore could be highly oxidized, leading to almost totally soluble polyglucuronic samples, while native cellulose (cellulose I) could only be partially

* Corresponding authors. Telephone: 33-476 03 76 14. Fax: 33-476 54 72 03. E-mail: (S.M.) suzelei.montanari@cermav.cnrs.fr; (M.R.V.) michel.vignon@cermav.cnrs.fr.

10.1021/ma048396c CCC: $30.25
Published on Web 02/11/2005

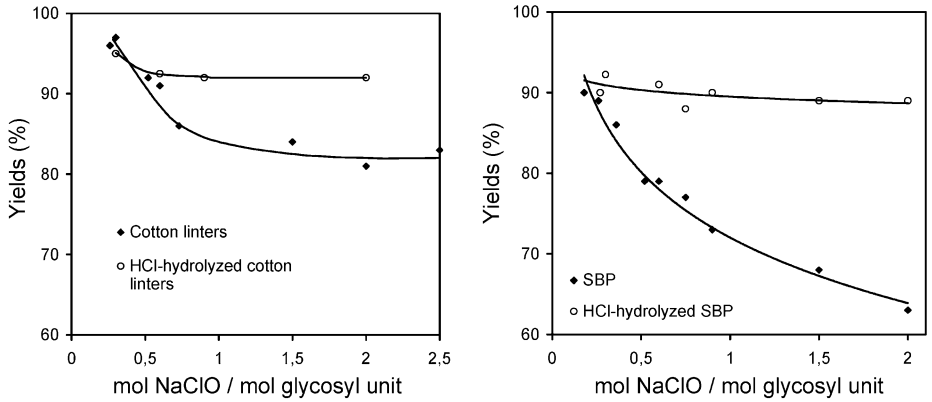

Figure 1. Molar yields of cotton linters and SBP carboxylated nanocrystals plotted versus the amount of added NaClO. Molar yield of carboxylated crystals was calculated using the carboxyl content (DO) values measured by conductimetry.

converted, due to its higher crystallinity and therefore the poor accessibility of primary hydroxyl groups.[25,28] This feature seems favorable for our present purposes, which is on one hand to introduce carboxyl groups at the surface of the crystals and on the other to compare the extent of oxidation of two different substrates of different crystallinity. This comparison should give some information about the number of accessible primary hydroxyl groups as a function of crystal size. The characterization of oxidized crystals could also give information about the cellulose surface and about the topochemistry of the TEMPO-oxidation reaction. The carboxylated nanocrystals were characterized by transmission electron microscopy (TEM) and solid state ^{13}C CP/MAS NMR and analyzed in terms of carboxyl content by conductimetry.

Experimental Procedures

Materials. Two cellulose samples were used in this work, cotton linters from Tubize Plastics, Rhodia (Belgium), and dried SBP from Saint Louis Sucre (Nassandres, France). Cotton linters were used as received, while SBP was purified according to the procedure of Dinand et al.[14]

Preparation of SBP Suspensions. Purified SBP samples were dispersed in water and disrupted in a Waring Blender operated at full speed for 5 min at a concentration between 1 and 2%. The slurry that had reached a temperature of 60 °C was immediately treated in a laboratory scale Manton−Gaulin homogenizer 15MR-8TBA, from APV Gaulin Inc., Wilmington, MA. Fifteen passes were applied at a pressure of 500 bar, and the temperature was kept below 95 °C to avoid cavitation. The resulting creamy suspension was freeze-dried or kept at 3−4 °C for further use.

HCl Hydrolysis. Twenty grams of cotton linters or 16 g of SBP were hydrolyzed with 1 L of 2.5 M HCl at 100 °C for 20 min. The hydrolyzate was filtered and washed with water until neutral pH.

Oxidation. Oxidation experiments were carried out as previously published with minor modifications.[25] In a typical run, cellulose samples (0.648 g, 4 mmol glycosyl units) were dispersed in distilled water (60 mL) for 3 min with a high-speed T25 basic Ultra-Turax homogenizer (Ika-Labortechnik, Staufen, Germany). The homogenizer was rinsed with 30 mL of water, which was collected and added to the cellulose suspension. TEMPO (10 mg, 0.065 mmol) and NaBr (0.21 g, 2 mmol) were added to the cellulose suspension, which was stirred magnetically and maintained at 20 °C. The NaClO was added dropwise to maintain the pH at 10 during the addition. After the total addition of NaClO, the pH was maintained constant at 10 by adding 0.5 M NaOH solution until no more variation was observed, indicating that the reaction was finished. Methanol (5 mL) was then added to react with the excess of NaClO and the pH was adjusted to 7 with 0.5 M HCl. After centrifugation, the supernatant, containing the water-soluble oxidized cellulose, was separated from the water-insoluble fraction. The supernatant, referred to as the soluble fraction, was dialyzed and freeze-dried. The water-insoluble fraction was resuspended in water and dialyzed to obtain the crystal suspensions.

Conductimetry. The carboxyl content of oxidized cellulose samples was determined by conductometric titrations.[25] The cellulose samples (30−40 mg) were suspended into 15 mL of 0.01 M hydrochloric acid solution. After 10 min of stirring, the suspensions were titrated with 0.01 M NaOH. The titration curves showed the presence of strong acid, corresponding to the excess of HCl and weak acid corresponding to the carboxyl content.

Transmission Electron Microscopy (TEM). The samples were deposited on carbon coated electron microscope grids and negatively stained with uranyl acetate. The grids were observed with a Philips CM200 CRYO TEM operated at an acceleration voltage of 80 kV.

Solid-State NMR. The NMR experiments were performed on a Bruker MSL spectrometer operating at a ^{13}C frequency of 50 MHz using the combined technique of proton dipolar decoupling (DD), magic angle spinning (MAS), and cross-polarization (CP). ^{13}C and ^{1}H field strengths of 64 kHz were used for the matched spin-lock cross-polarization transfer. The spinning speed was set at 3000 Hz for all the samples. The contact time was 1 ms, the acquisition time 70 ms, and the recycle delay 4 s. The deconvolution of the spectra was achieved following earlier procedure.[16] The position and width of the lines were maintained constant throughout a series of samples. The area corresponding to the integration of the C1 signal was set to one. The evaluation of the oxidation and crystallinity degree was made from the integration of the corresponding deconvoluted lines.

Results and Discussion

Yield in Oxidized Crystals and Soluble Products. In the TEMPO-oxidation experiments of cotton linters and SBP, two fractions were obtained after centrifugation. The supernatant was entirely water-soluble and consisted of totally oxidized polyglucuronans,[25] whereas the insoluble material corresponded to surface carboxylated cellulose crystals. The molar yields of soluble fraction increased with the amount of NaClO, to a maximal value of around 14% for cotton linters and 24% for SBP. Accordingly, the yield of oxidized crystals decreased with increasing amount of NaClO and dropped to constant values, namely, almost 81% for cotton linters and 63% for SBP (Figure 1).

The oxidation of HCl hydrolyzed cotton linters and SBP led to slightly different results as the acid hydrolysis had already removed the amorphous zones from the starting material. In this work, the hydrolysis yields

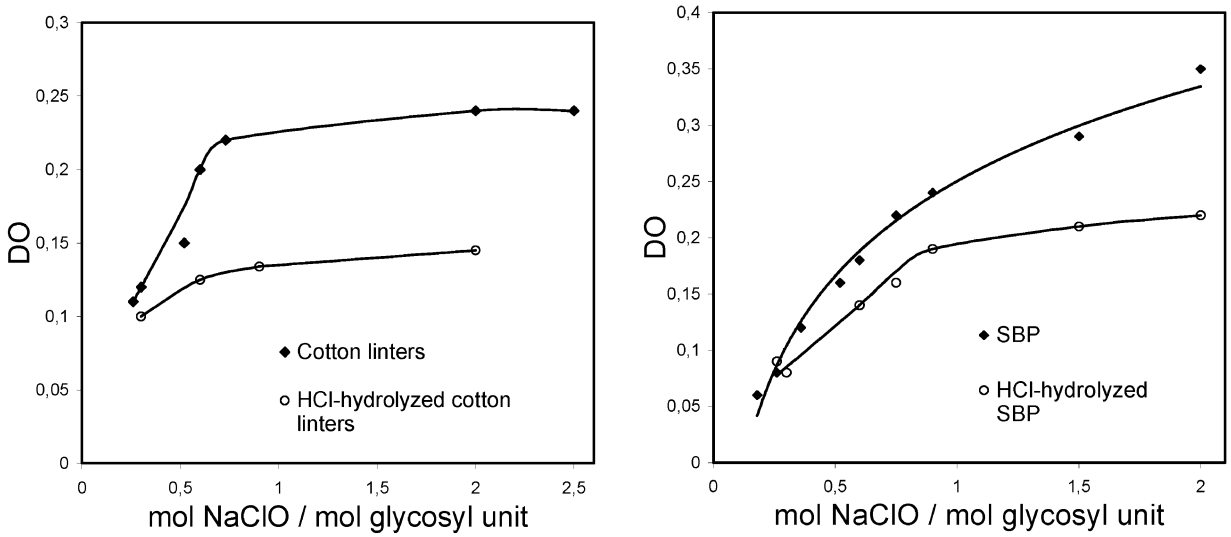

Figure 2. Degree of oxidation (obtained by conductimetry) of cotton linters and SBP carboxylated nanocrystals vs the amount of added NaClO.

were around 90% for cotton linters and 75−80% for SBP. Concerning the microfibrillated SBP samples, we observed that during the hydrolysis treatment, 20−25% of the material was solubilized. This product loss seems to correspond to the hydrolysis of the amorphous zones and to the removal of the residual hemicellulose and pectic polysaccharides located at the surface of the microfibrils.[16,17] The hydrolyzed samples were oxidized by the TEMPO method with variable quantities of NaClO, and we obtained approximately constant molar yields of soluble fractions, namely, 4−7% in the case of cotton linters and 7−11% with microfibrillated SBP. The amount of oxidized crystals was also more or less constant (i.e., 92−95% with cotton linters and 88−92% with microfibrillated SBP).

In the case of nonhydrolyzed samples, the crystals yields were lower than in the case of the hydrolyzed samples. This difference could be explained by a preferential oxidation in the amorphous domains, where higher amounts of primary hydroxyl groups were oxidized and partial solubilization could occur. In contrast, the yields were higher when the amorphous zones of the samples had been preliminary removed by acid hydrolysis.

The global yields for hydrolyzed samples were always between 98 and 100%, whereas for nonhydrolyzed samples this values decreased slightly with increasing quantities of NaClO to values around 95% for cotton linters. In the case of microfibrillated SBP, the decrease of global yield was more pronounced to reach values inferior to 90%. This loss of material can be explained by the degradation of oxidized cellulose and is more important when the soluble fraction is high, as in the case of microfibrillated SBP.

Degree of Oxidation (DO). The carboxyl content of oxidized cellulose samples was determined by conductometric titrations. The sodium cations bound to the carboxyl groups were exchanged by hydrogen ions through treatment with an excess of hydrochloric acid. We carried out a direct titration with alkali, and the titration curves showed the presence of a strong acid, corresponding to an excess of HCl and a weak acid, corresponding to the carboxyl content. The DO was calculated as already published,[25] and very reproducible results were obtained.

We observed that the DO increased with the NaClO concentration (Figure 2) to a maximal value that depends on the crystal size and corresponds grossly to the amount of primary hydroxyl groups easily accessible to the reactants. The maximal DOs were around 0.15 and 0.23 for HCl-hydrolyzed cotton linters and SBP, respectively. In the case of nonhydrolyzed samples, we observed higher maximal DO, about 0.23 for cotton linters and 0.35 for SBP (Figure 2).

TEM Analysis. Electron micrographs of the oxidized cellulose samples are presented in Figures 3 and 4. In these pictures, the negative stain reveals the individual crystals that have diameters of the order of 4−5 nm for cotton samples and 3−4 nm for those of SBP. These crystals are highly aggregated in the hydrolyzed samples (Figures 3c and 4c), as well as the samples of low degree of oxidation (Figures 3a and 4a), but the aggregates tend to be thinner in the most oxidized specimens (Figures 3b,d and 4b,d). Nevertheless, in these latter cases, isolated crystals are rarely seen as the samples consist rather of crystallites made of two or three individual crystals. An other aspect of the crystallites in Figures 3d and 4d is that they have sharp contours, both at their side and at their tips, indicating therefore that there is no dangling carboxylated chains partially hooked to the crystals and partially floating in the surrounding medium. The better individualization of the crystals resulting from the increase in oxidation can be explained by the electrostatic repulsion of the negatively charged carboxyl groups located at the surface of the crystals. In the case of nonhydrolyzed cotton linters and microfibrillated SBP samples, the TEMPO-mediated oxidation induced cleavages in the amorphous zones; thus, the long microfibrils are drastically cut to yield crystallites that tend to have the same appearance as those of the acid hydrolyzed specimens (Figures 3b and 4b). During the HCl-hydrolysis of cotton linters and microfibrillated SBP, amorphous domains were removed, and crystals aggregates were obtained (Figures 3c and 4c). The surface oxidation improved the individualization of the crystals (Figures 3d and 4d). A comparison of Figures 3d and 4d with, respectively, those of Figures 3b and 4b suggests that the hydrolyzed and oxidized SBP crystals tend to be longer and thinner than the

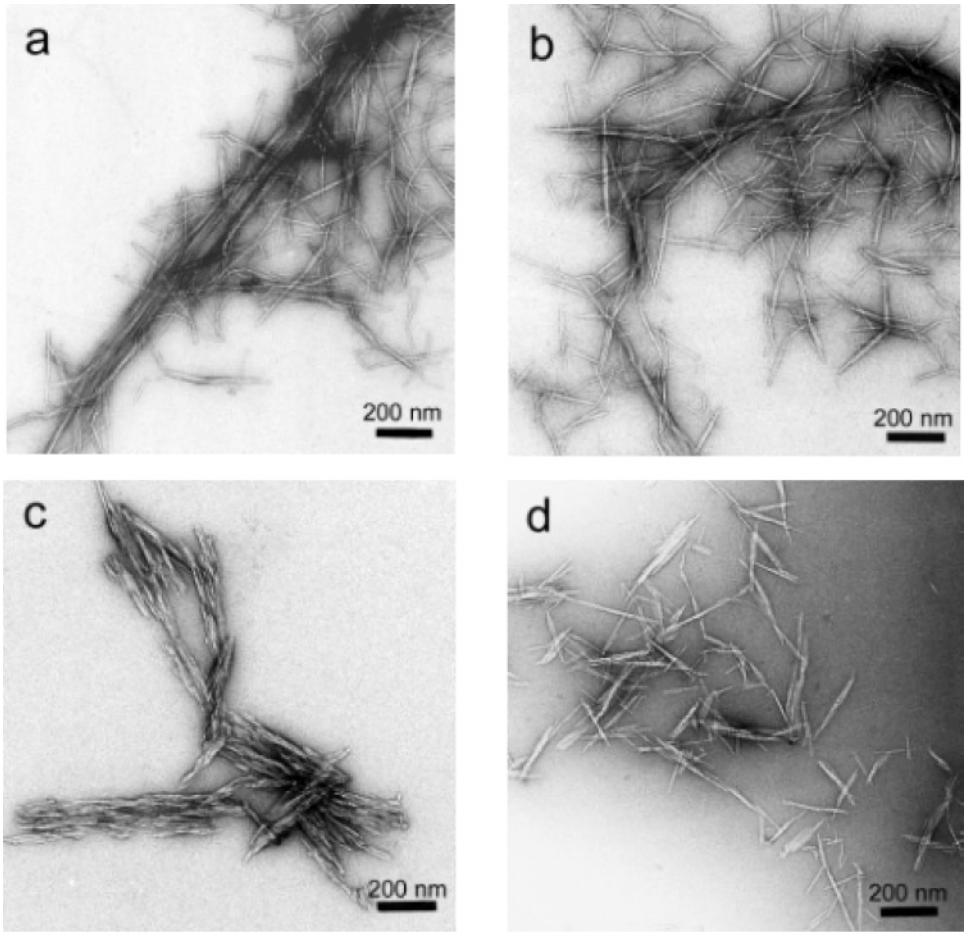

Figure 3. TEM of cellulose crystals from cotton linters origin: (a) partially oxidized cotton linters (0.36 mol NaClO/mol glycosyl unit); (b) oxidized cotton linters (1.5 mol NaClO/mol glycosyl unit); (c) HCl-hydrolyzed cotton linters; and (d) HCl-hydrolyzed and oxidized cotton linters (0.9 mol NaClO/mol glycosyl unit).

corresponding hydrolyzed and oxidized cotton linters samples.

Solid State NMR. The samples obtained by TEMPO-mediated oxidation were characterized by solid-state NMR and the CP-MAS spectra obtained prior and after oxidation are shown in Figures 5 and 6.

The spectra obtained on the starting raw samples have already been described in the literature.[16,29] The spectrum of the cotton linter sample shows the lowest contribution of the disordered regions centered at 83.5 and 62.4 ppm for the C4 and C6 carbons, respectively, as compared to the SBP sample, in accordance with its higher crystallinity and/or crystallite size. Similarly, the contribution of the disordered regions is lower for the hydrolyzed SBP samples than for the nonhydrolyzed ones. The same trend has already been observed during the purification process of SBP samples and is likely due to the removal of disordered chains and/or residual surface hemicelluloses.[16]

Upon oxidation, the major change is the appearance of a signal at 174.8 ppm corresponding to the carboxyl groups. As already observed by conductometric titration, the amplitude of this signal is higher for SBP samples than for the cotton samples and higher for the crude samples than for the hydrolyzed ones. At the same time, one observes a decrease in the intensity of the signal at 62.4 ppm, corresponding to the carbons of the primary hydroxyl groups (C6) of the disordered regions. To go further into details, the integration of the most relevant signals has been achieved. The results are given in Table 1, together with their integration data. The DO was evaluated by the integration of the signal at 174.8 ppm. A crystallinity index can be estimated by the comparison of the surface area of C4 signals at 83.5 and 88.7 ppm corresponding to the carbons in disordered and crystalline regions, respectively.[16]

Table 1 reveals that the carboxyl group content increases with the amount of NaClO and that there is a good agreement with the DO values resulting from NMR and those obtained by conductimetry. At the same time, the amount of primary hydroxyl groups at the surface and in amorphous domains decreased, but residual amorphous primary hydroxyl group signals are still present in small amounts. Conversely, a remarkable decrease of the C6 signal at 62.5 ppm corresponding to the disordered part is observed during the course of the oxidation process, whereas the crystalline contribution at 65 ppm remains constant. Thus, the onset of this carboxyl contribution arises at the unique expense of the amorphous C6 contribution. This observation is a strong indication that only the primary hydroxyl groups are oxidized and that for the insoluble part, this oxidation occurs only in the disordered regions of the sample.

As already stated by observation of Figures 5 and 6, cotton linters have a higher crystallinity index than SBP, according to the small size of SBP crystals. The comparison of nonhydrolyzed and hydrolyzed samples confirmed the removal of some of the disordered contribution by the HCl hydrolysis, as can be observed by

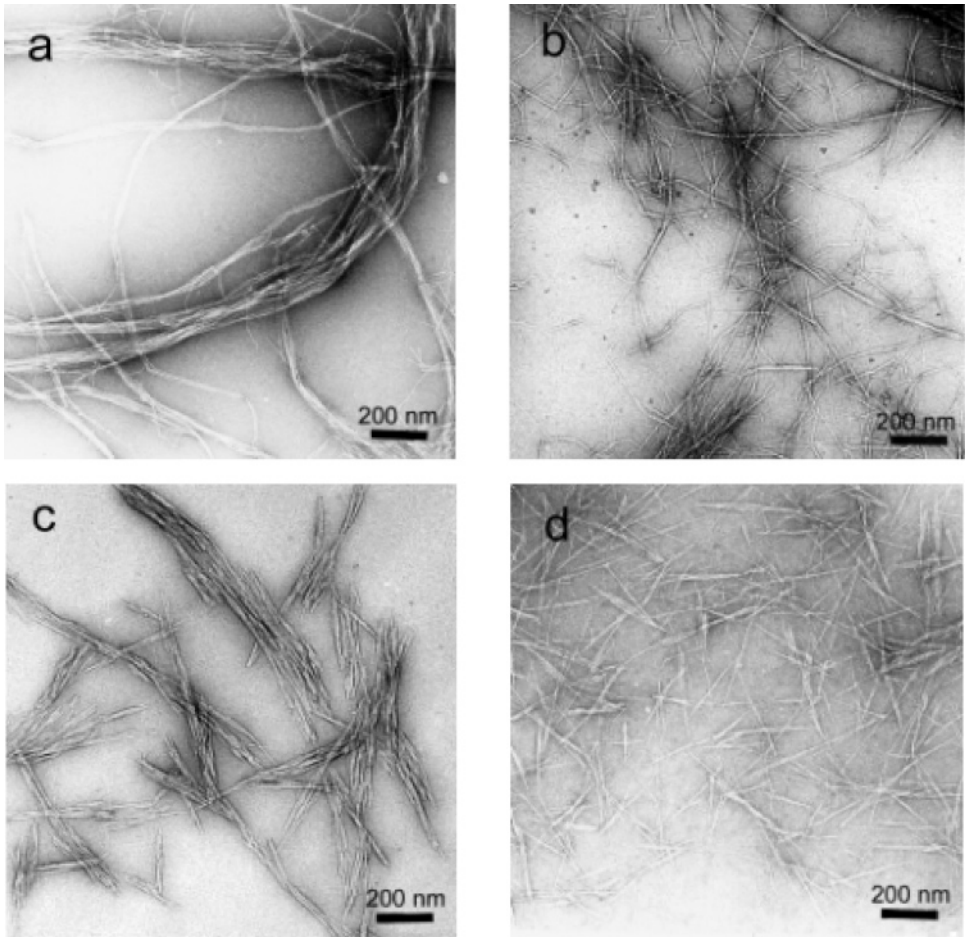

Figure 4. TEM of cellulose crystals from SBP origin: (a) oxidized SBP (0.18 mol NaClO/mol glycosyl unit); (b) oxidized SBP (0.9 mol NaClO/mol glycosyl unit); (c) HCl-hydrolyzed SBP; and (d) HCl-hydrolyzed and oxidized SBP (0.9 mol NaClO/mol glycosyl unit).

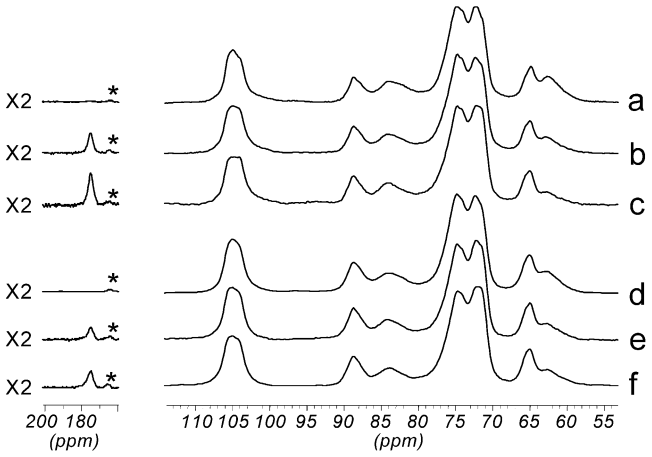

Figure 5. CP-MAS Carbon-13 NMR spectra of microfibrillated SBP: (a) original sample; (b) oxidized SBP (0.75 mol NaClO/mol glycosyl unit); (c) oxidized SBP (2 mol NaClO/mol glycosyl unit); (d) HCl-hydrolyzed; (e) HCl-hydrolyzed and oxidized (0.75 mol NaClO/mol glycosyl unit; (f) HCl-hydrolyzed and oxidized (2 mol NaClO/mol glycosyl unit). The spectral region corresponding to the C=O signals (175−200 ppm) has been multiplied by a factor 2. Asterisks (*) indicate residual spinning sidebands from the C1 signal.

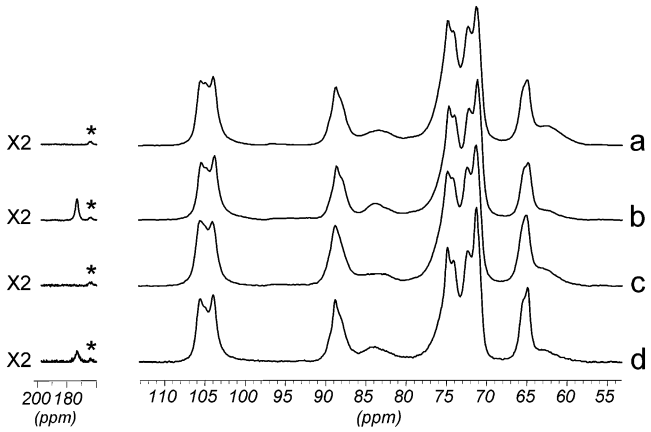

Figure 6. CP-MAS Carbon-13 NMR spectra of cotton linters: (a) original sample; (b) oxidized (2 mol NaClO/mol glycosyl unit); (c) HCl-hydrolyzed; and (d) HCl-hydrolyzed and oxidized (2 mol NaClO/mol glycosyl unit). The spectral region corresponding to the C=O signals (175−200 ppm) has been multiplied by a factor 2. Asterisks (*) indicate residual spinning sidebands from the C1 signal.

the decrease of the C4 signal contribution in disordered regions for hydrolyzed samples. This general trend is conserved throughout the samples, either before or after oxidation. It is, however, worth noting that the crystallinity index does not evolve during the oxidation process. This latter observation is a strong indication that the integrity of the crystallites is not altered by the oxidation.

Oxidized Crystals. To try to rationalize the oxidation results obtained in this study, one must consider the organization of cellulose in plant cell walls. According to current models,[30,31] cellulose is believed to consist of assemblies of slender crystalline microfibrils more or less aggregated. Following the work of Revol[32] on

Table 1. Results of the Quantitative Analysis of CP-MAS Carbon-13 NMR Spectra

cellulose samples	NaClO (molar ratio)[a]	C=O[b] (174.8 ppm)	C6*cryst*[c] (68−63 ppm)	C6*amor*[c] (63−58 ppm)	C6*total*[d] (68−58 ppm)	C4*cryst*[c] (*CI*[e]) (91−86 ppm)	C4*amor*[c] (86−81 ppm)
SBP	0	0	0.46	0.53	0.99	0.44	0.58
SBP	0.75	0.28	0.42	0.27	0.69	0.47	0.52
SBP	2	0.38	0.46	0.13	0.59	0.47	0.53
hydrolyzed SBP	0	0	0.54	0.38	0.92	0.52	0.51
hydrolyzed SBP	0.75	0.15	0.53	0.26	0.75	0.50	0.48
hydrolyzed SBP	2	0.22	0.53	0.25	0.78	0.52	0.44
cotton linters	0	0	0.54	0.37	0.92	0.69	0.33
cotton linters	2	0.27	0.58	0.16	0.74	0.70	0.28
hydrolyzed cotton linters	0	0	0.68	0.22	0.90	0.75	0.25
hydrolyzed cotton linters	2	0.10	0.68	0.13	0.81	0.72	0.28

[a] Mol NaClO/mol gycosyl unit. [b] Carboxyl groups (DO) obtained by integration of the signal at 174.8 ppm. [c] Crystalline and amorphous contents determined by deconvolution. [d] Obtained by integration of the signal at 62.4 ppm. [e] Crystallinity index.

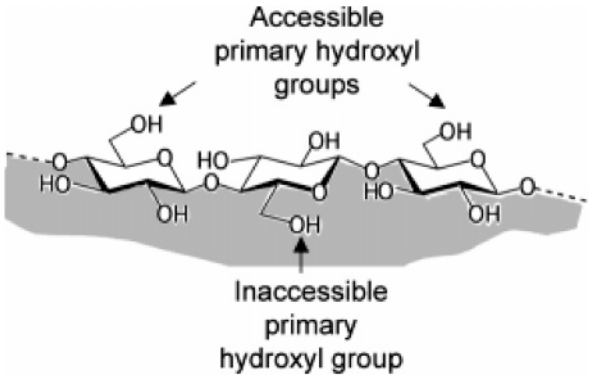

Figure 7. Schematic drawing of a cellulose chain at the surface of a cellulose crystal.

Valonia cellulose, it is frequently assumed that the cellulose microfibrils have square section with exposed surfaces corresponding to the (110) and (1$\bar{1}$0) crystal planes of the cellulose lattice (in this work, we refer to the cellulose unit cell defined by Sugiyama et al.)[33] As opposed to the core of the microfibrils, which is considered to be in a crystalline arrangement, the microfibril surfaces are organized in a different manner since the surface chains are not taken in a three-dimensional network. The difference between surface and core chains is clearly evidenced in CP/MAS ^{13}C NMR spectra of cellulose where different resonances at C4 are attributed either to the core or surface cellulose chains.[16,34−37] Regarding the surface chains, one distinguishes accessible surfaces that are located at the exterior of microfibrils aggregates and are therefore accessible to oxidation and inaccessible surfaces that are located inside the microfibrils aggregates. In addition, the cellulose microfibrils contain a number of defects, such as twists,[3] chain ends, and kinks that are partially hydrolyzed by acid, leading to the conversion of microfibrils into nanocrystals aggregates.

Our oxidation results on hydrolyzed samples have shown that the oxidation took place only at the surface hydroxymethyl groups. Regarding the description of the (110 and 1$\bar{1}$0) surfaces of a given crystal, only one-half of the surface hydroxymethyl are accessible to the oxidation, the other half being buried toward the core of the crystalline domains (Figure 7). This assumption is in good agreement with the solid-state NMR results (Table 1). Indeed, for the hydrolyzed samples, the amount of nonoxidized hydroxymethyl groups in the disordered regions (C6*amor*) is very close to that of the carboxyl group in the completely oxidized samples, with values of, respectively, 0.25 and 0.22 for SBP and 0.13 and 0.10 for cotton linters. These figures correspond roughly to half of the C4*amor* content determined for these samples. These data suggest that when both samples are totally oxidized, the residual signal at 62.4 ppm (C6*amor*) corresponds to surface primary hydroxyl groups directed toward the interior of the crystal and thus inaccessible to the TEMPO-oxidation method. Thus, if a fully oxidized individual nanocrystal is considered, its DO can be correlated with its lateral size, assuming a square section for such element. If n is the number of cellulose chains per side of the crystal, n^2 will be the number of chains in the crystal. The number of chains in the crystalline core of the crystal is $(n - 2)^2$, and the number of surface chains is $4(n - 1)$.

The ratio (r) of surface chains to the total number of cellulose chains in the crystal can be calculated by the following equation:

$$r = \frac{4(n-1)}{n^2} \tag{1}$$

which gives

$$n = 2\frac{1+\sqrt{1-r}}{r} \tag{2}$$

Assuming that the maximal DO is relative only to the surface oxidation and that only every second surface hydroxymethyl group can be oxidized, the following relation can be obtained:

$$\mathrm{DOmax} = \frac{r}{2} \tag{3}$$

From the values of DO max for hydrolyzed cotton linters (DO = 0.15) and SBP (DO = 0.23), we can deduce that n is between 7 and 8 for hydrolyzed SBP and 12 for hydrolyzed cotton. Taking an average value of 0.57 nm between cellulose chains within the (110) and (1$\bar{1}$0) faces of the crystal, we obtain a value of 4.2 nm for the width of a SBP crystal and 6.8 nm for the corresponding crystal of cotton linter. These values correspond roughly to the average sizes of the crystallites observed in Figures 3d and 4d. Obviously, if the cellulose nanocrystals are aggregated into larger crystallites and if only the crystallite surfaces were accessible, the calculation for the value of the widths of the individual crystals would yield smaller numbers. On the other hand, if the microfibrils did not have square section, but had shapes where more hydroxymethyl groups were exposed, these calculations should be modified to account for such morphology.

Another independent method to calculate the width of the crystalline domains in cellulose is based on ^{13}C solid-state NMR data, using the so-called crystallinity index (CI), which is obtained by comparing the intensity of the C4 signal corresponding to the crystalline part, with the total signal at this carbon.[16,34] Assuming again a square section for the crystals, CI is correlated with n as follows:

$$\mathrm{CI} = \left(\frac{n-2}{n}\right)^2 \tag{4}$$

which gives

$$n = 2\frac{1+\sqrt{\mathrm{CI}}}{1-\mathrm{CI}} \tag{5}$$

Taken from Table 1, the values of CI are 0.52 for hydrolyzed SBP and 0.75 for hydrolyzed cotton linters. Thus, from NMR results, values of n are of 7 for SBP and 15 for hydrolyzed cotton linters. Thus, at first instance, there is a close agreement between the values of the width of the crystals, calculated from conductometric data on fully oxidized crystals and those resulting from NMR measurements on the hydrolyzed crystals, before oxidation. Analyzing this agreement, it seems that on one hand the full oxidation did not reduce the width of the cellulose crystals and that on the other, the oxidized crystals are no longer aggregated since all surfaces are oxidized.

Despite this agreement, an inspection of the micrographs of the hydrolyzed and oxidized crystals in Figures 3d and 4d reveals some aggregation as most of the elements seen in these figures are in fact crystallites consisting of two or three individual crystals. Thus, there is some discrepancy between these observations and the smaller crystal widths deduced from either conductometric or NMR data. Several reasons can be brought to account for this difference. The most logical is that the square microfibril model with (110) and ($1\bar{1}0$) surfaces, which has been established for *Valonia* and algal cellulose, may not apply at all for cotton linters and SBP microfibrils. Indeed, if the microfibrils or nanocrystals had surfaces other than (110) and ($1\bar{1}0$), and if their sections were not square, it could be that all surface hydroxymethyl group could be oxidized, instead of one out of two, as shown in Figure 7. If this is the case, a model with crystallites consisting of an association of two crystals would establish a fit between the NMR and the conductometric data. Other possibilities, which would reconcile our ultrastructural observations with the spectroscopic and conductometric results, would be that some hydroxymethyl groups located beneath the crystal surface have also been oxidized. In view of these uncertainties, it seems better to leave this analysis open until a good molecular description of the surface of cellulose crystals is firmly established.

The aqueous suspensions of the oxidized crystals did not flocculate or sediment. When observed between cross polarizers, dilute suspensions presented a marked birefringence indicative of the presence of domains where the crystallites are aligned parallel to one another. Upon concentrating these suspensions, it was not possible, so far, to reach chiral−nematic states that are classically observed with cellulose crystallites prepared with sulfuric acid.[9] This lack of organization may be due to a too large polydispersity of the oxidized crystallite lengths or to other effects that are specific of the TEMPO oxidation.

Acknowledgment. The authors acknowledge the help of I. Paintrand for the TEM pictures and Dr. H. Chanzy for valuable discussion during this work. M.R. was a recipient of CNRS-Lebanon fellowship.

References and Notes

(1) Gardner, K. H.; Blackwell, J. *Biopolymers* **1974**, *13*, 1975−2001.
(2) Brown, R. M., Jr. *J. Macromol. Sci. Pure Appl. Chem.* **1996**, *A33(10),* 1345−1373.
(3) Willison, J. H. M.; Abeysekera, R. M. In *Botanical Microscopy*; Robards, A. W., Ed.; Oxford University Press: Oxford, 1985; pp 181−203.
(4) Battista, O. A. *Ind. Eng. Chem.* **1956**, *48*, 333−335.
(5) Mukherjee, S. M.; Woods, H. J. *Biochim. Biophys. Acta* **1953**, *10*, 499−511.
(6) Orts, W. J.; Godbout, L.; Marchessault, R. H.; Revol, J.-F. *Macromolecules* **1998**, *31*, 5717−5725.
(7) Dong, X. M.; Gray, D. G. *Langmuir* **1997**, *13*, 2404−2409.
(8) Marchessault, R. H.; Morehead, F. F.; Walter, N. M. *Nature* **1959**, *184*, 632−633.
(9) Revol, J.-F.; Bradford, H.; Giasson, J.; Marchessault, R. H.; Gray, D. G. *Int. J. Biol. Macromol.* **1992**, *14*, 170−172.
(10) Revol, J.-F.; Godbout, L.; Dong, X. M.; Gray, D. G.; Chanzy, H.; Maret, G. *Liquid Cryst.* **1994**, *16*, 127−134.
(11) Dong, X. M.; Revol, J.-F.; Gray, D. G. *Cellulose* **1998**, *5*, 19−32.
(12) Araki, J.; Wada, M.; Kuga, S.; Okano, T. *Colloids Surf. A* **1998**, *142*, 75−82.
(13) Araki, J.; Wada, M.; Kuga, S.; Okano, T. *J. Wood Sci.* **1999**, *45*, 258−261.
(14) Dinand, E.; Chanzy, H.; Vignon, M. R. *Food Hydrocolloids* **1999**, *13*, 275−283.
(15) Dinand, E.; Chanzy, H.; Vignon, M. R. *Cellulose* **1996**, *3*, 183−188.
(16) Heux, L.; Dinand, E.; Vignon, M. R. *Carbohydr. Polym.* **1999**, *40*, 115−124.
(17) Dinand, E.; Vignon, M. R. *Carbohydr. Res.* **2001**, *330*, 285−288.
(18) Araki, J.; Wada, M.; Kuga, S.; Okano, T. *Langmuir* **2000**, *16*, 2413−2415.
(19) Araki, J.; Wada, M.; Kuga, S. *Langmuir* **2001**, *17*, 21−27.
(20) Davis, N. J.; Flitsch, S. L. *Tetrahedron Lett.* **1993**, *34*, 1181−1184.
(21) de Nooy, A. E.; Besemer, A. C.; van Bekkum, H. *Recl. Trav. Chim. Pays-Bas* **1994**, *113*, 165−166.
(22) de Nooy, A. E.; Besemer, A. C.; van Bekkum, H. *Carbohydr. Res.* **1995**, *269*, 89−98.
(23) de Nooy, A. E.; Besemer, A. C.; van Bekkum, H.; van Dijk, J. A. P. P.; Smit, J. A. M. *Macromolecules* **1996**, *29*, 6541−6547.
(24) Bragd, P. L.; van Bekkum, H.; Besemer, A. C. *Top. Catal.* **2004**, *27*, 49−66.
(25) da Silva Perez, D.; Montanari, S.; Vignon, M. R. *Biomacromolecules* **2003**, *4*, 1417−1425.
(26) Tahiri, C.; Vignon, M. R. *Cellulose* **2000**, *7*, 177−188.
(27) Isogai, A.; Kato, R. H. *Cellulose* **1998**, *5*, 153−164.
(28) Saito, T.; Isogai, A. *Biomacromolecules* **2004**, *5*, 1983−1989.
(29) Horii, F.; Yamamoto, H.; Kitamaru, R.; Tanahashi, M.; Higuchi, T. *Macromolecules* **1987**, *20*, 2946−2949.
(30) Preston, R. D. *The Physical Biology of Plant Cell Walls*; Chapman & Hall: London, 1974.
(31) Roelofsen, P. A. *The Plant Cell-Wall*; Gebrüder Borntraeger: Berlin-Nikolasee, 1959.
(32) Revol, J.-F. *Carbohydr. Polym.* **1982**, *2*, 123−134.
(33) Sugiyama, J.; Vuong, R.; Chanzy, H. *Macromolecules* **1991**, *24*, 4168−4175.
(34) Newman, R. H. *Solid State Nucl. Magn. Reson.* **1999**, *15*, 21−29.
(35) Larsson, P. T.; Wickholm, K.; Iversen, T. *Carbohydr. Res.* **1997**, *302*, 19−25.
(36) Wickholm, K.; Larsson, P. T.; Iversen, T. *Carbohydr. Res.* **1998**, *312*, 123−129.
(37) Atalla, R. H.; VanderHart, D. L. *Solid State Nucl. Magn. Reson.* **1999**, *15*, 1−19.

MA048396C